

## PREPARATION AND APPLICATION PROPERTIES OF Ti-Si GLYCOL SALT CATALYSTS FOR POLYESTERS

Yang Yu<sup>a</sup>, Guoliang Shen<sup>a,\*</sup>, Tie jun Xu<sup>a</sup>, Ruiyang Wen<sup>a</sup>, Yong jie Wang<sup>a</sup>, Yue Huo<sup>a</sup> and Shi jie Xu<sup>a</sup><sup>a</sup>Shenyang University of Technology, 111003 Liaoyang, China

Received: 11/04/2023; accepted: 02/01/2024; published online: 04/16/2024

Silicon catalysts have very low catalytic activity in polyester (PET). However, titanium catalysts have high catalytic activity in polyester. The simultaneous use of titanium and silicon catalysts is effective in reducing the activity of a single titanium catalytic base agent. In addition, the glycol salts of titanium and silicon (Ti-EG and Si-EG) prepared in the present invention for use in the polyester catalytic process can avoid the introduction of other groups of impurities during the polyester catalytic process, which would lead to premature capping of the polyester in the process of polycondensation and chain building and make it difficult to increase the molecular weight, and thus affect the quality of the polyester. It has been verified that the ratio of Ti:Si is 1:1 (mol), and total amount added to the catalyst is 0.15% of the raw material amount, and the polycondensation temperature was 260-280 °C for 60 min. Compared with the single Ti-EG catalyst, the  $\eta_{inh}$  value of the synthesized PET was significantly reduced, and the molecular weight and other indexes did not change too much. In addition, at the end of catalysis, the catalyst was uniformly dispersed in the reaction system, which could be used as a matting agent for PET.

Keywords: catalyst; polymerization; polyester; activity.

## INTRODUCTION

Polyethylene terephthalate (PET) is currently the world's largest-produced product and the most widely used polyester material in food packaging, clothing, electrical products, electronics, automobiles, machinery, fast-moving consumer goods and other aspects of life.<sup>1-3</sup> In PET industrial production, the catalysts used can be divided into antimony,<sup>4</sup> titanium,<sup>5-8</sup> aluminum,<sup>9,10</sup> and germanium.<sup>11</sup> At present, more than 90% of the catalysts used in the industrial synthesis of polyester are antimony-based, but they are potentially toxic to the environment and organisms, so more and more research focuses on titanium-based catalysts, which are catalytically high active,<sup>12-15</sup> environmentally friendly, and inexpensive. It is used to replace traditional antimony-based polyester catalysts. However, studies have shown that Ti has a strong Lewis acidity due to its shell electron arrangement which makes it electron-deficient in its layer orbitals. This caused titanium catalysts to have very high catalytic activity, and a yellowish color of polyester production, which limits their large-scale application. Therefore, it is urgent to prepare titanium polyester catalysts with moderate catalytic activity, good dispersion, and stable catalytic performance.

In this paper, Si, which is abundant in nature, non-toxic, harmless, cheap, and easily available, was chosen to be used in combination with Ti.<sup>16-23</sup> Glycol salts of titanium and silicon (Ti-EG, Si-EG) were prepared separately for use as catalysts in the synthesis of PET. Compared with the previous study,<sup>24</sup> this study also investigated the catalytic performance of Ti-EG and Si-EG applied alone and mixed together, explored the optimal ratio of the two catalysts under the same application conditions, and analyzed the catalytic performance of the catalysts under different ratios. As glycol salts does not lead to the introduction of impurities at the polyester polycondensation stage and avoids the difficulties in the chain-building process due to impurities, this is favorable for polyester molecular weight increase.<sup>25-31</sup> Due to the arrangement of the extra-nuclear electron cloud of Si, its catalytic activity is very weak when it is used alone, and using it together with Ti can play a role in decreasing the catalytic activity of Ti, and the

deactivated catalyst is evenly dispersed in PET after the end of the catalytic process of Ti-EG, Si-EG, and it can be used as a matting agent which will not affect the quality of the product.<sup>32,33</sup>

## EXPERIMENTAL

## Materials and instruments

## Materials

Butyl titanate (Damao Chemical Reagent Factory, Tianjin, China); tetraethyl silicate (Aladdin Reagent Co., Shanghai, China); xylene (Damao Chemical Reagent Factory, Tianjin, China); anhydrous ethanol (Maclean's Biochemical Technology Co., Shanghai, China); terephthalic acid (PTA) (Damao Chemical Reagent Factory, Tianjin, China); ethylene glycol (EG) (Maclean's Biochemical Technology Co., Shanghai, China). The raw materials used in the experiments were all analytically pure reagents.

## Instruments

A balance FA2204B (China Shanghai Precision Scientific Instruments, Shanghai, China); viscometer (Lianghe glass meter, China); field emission scanning electron microscope Regulus SU8230 (Hitachi, Japan); infrared spectrometer TENROR-II (Bruker, Germany); thermogravimetric analyzer STA 449 F3 (Bruker, Germany); X-ray diffraction spectrometer D8 Advance (Bruker, Germany); differential scanning calorimeter 822e (Mettler Toledo, Switzerland); colorimeter ADCI-60-C (Cintec Instrument Technology Co., China); circulating water vacuum pump SHZ-D (Ruide Instrument & Equipment Co., China); laser particle size distribution meter BT-800 (Baxter Instruments Co., China).

## Methods

## Catalyst preparation

Tetraethyl silicate and ethylene glycol were introduced into xylene, with the xylene amount being 0.8-1.5 times the total mass of the raw materials. The mixture was then mixed and stirred. As the temperature was increased, the reaction distillate was collected. The

\*e-mail: shengl\_shxy@sut.edu.cn

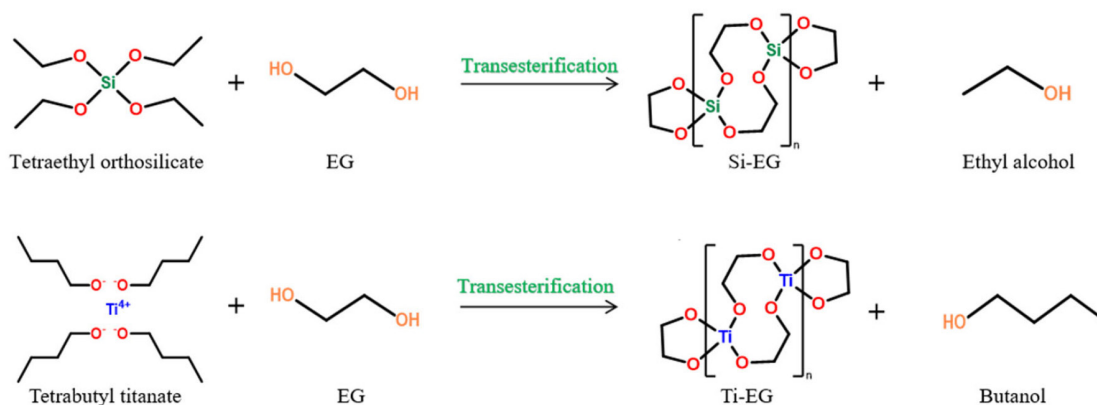


Figure 1. Preparation of Ti-EG and Si-EG catalysts

reaction was carried out at temperatures ranging from 90-120 °C for a duration of 5-8 h. After the reaction was completed, the solvent xylene was evaporated. The resulting product was crushed, washed with anhydrous ethanol, and dried to synthesize Si-EG.

Butyl titanate and ethylene glycol were added to xylene, with the amount of xylene being 0.8-1.5 times the total mass of the raw materials. The mixture was mixed and stirred. As the temperature was increased, the reaction distillate was collected. The reaction conditions were set at temperatures ranging from 120-140 °C for a period of 3-5 h. Upon completion of the reaction, the solvent xylene was evaporated. The resultant product was crushed, washed with anhydrous ethanol, and dried to synthesize Ti-EG.

The synthesis of Si-EG and Ti-EG catalysts is shown in Figure 1.

Si-EG: tetraethyl silicate undergoes an ester exchange reaction with ethylene glycol, in which the two hydroxyl groups at the ends of the ethylene glycol undergo an ester exchange reaction with ethyl (-CH<sub>2</sub>CH<sub>3</sub>) in tetraethyl silicate to form Si (-OCH<sub>2</sub>CH<sub>2</sub>O)<sub>2</sub> (Si-EG) and displace ethanol.

Ti-EG: butyl titanate undergoes an ester exchange reaction with ethylene glycol, in which the two hydroxyl groups at the ends of the ethylene glycol undergo an ester exchange reaction with the butyl group (-CH<sub>2</sub>CH<sub>2</sub>CH<sub>2</sub>CH<sub>3</sub>) in butyl titanate, generating Ti (OCH<sub>2</sub>CH<sub>2</sub>O)<sub>2</sub> (Ti-EG) and displacing the butanol.

#### Synthesis of PET

The synthesis steps of PET are shown in Figure 2, and the synthesis is divided into an esterification stage and a polycondensation stage.

Esterification reaction: hydroxyl groups in terephthalic acid (PTA) form water with hydrogen removed from hydroxyl groups in ethylene glycol (EG), while esterification produces ethylene glycol terephthalate.

Polycondensation reaction: the polycondensation step begins with the removal of hydroxyl (-OH) and hydroxyethyl (-CH<sub>2</sub>CH<sub>2</sub>OH) groups from each end of polyethylene terephthalate, respectively, which combine to form EG. Then the monomers that have been removed from both ends are joined to each other to form polyethylene

terephthalate with a low degree of polymerization ( $x = 1 \sim 4$  or so), which is the pre-condensation stage. In the polycondensation stage, the chain-building reaction is repeated under reduced pressure and high temperature to produce large molecular weight PET.

The raw material terephthalic acid (PTA) and ethylene glycol were added to the reactor, and the total amount of catalyst added was 0.015% of the raw material amount, and the catalyst was uniformly dispersed in the ethylene glycol before catalyst use. The esterification reaction was carried out under the conditions of atmospheric pressure, temperature between 185-195 °C, and stirring speed of about 100 r min<sup>-1</sup>. The polycondensation test was carried out under the conditions of temperature between 260-280 °C, stirring speed of 100 r min<sup>-1</sup>, and pressure of -0.1 MPa.

#### PET molecular weight testing

Tests for characteristic viscosity: the molecular weight parameters presented herein were obtained from a solvent mixture of phenol:tetrachloroethane of 1:1 (wt.%), tested in a constant temperature water tank at 25 °C using a Uhl's viscometer.

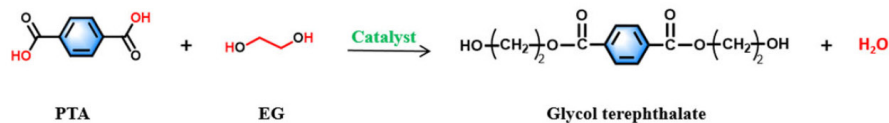
$$\eta_r = \frac{t - t_0}{t_0} \quad (1)$$

$$\eta_{sp} = \frac{t_1 - t_0}{t_0} = \eta_r - 1 \quad (2)$$

$$[\eta] = \frac{\sqrt{1 + 1.4\eta_{sp}} - 1}{0.7c} \quad (3)$$

According to Equations 1-3,  $\eta_r$  is the relative viscosity;  $t_1$  is the solution's flow time through the capillary (s);  $t_0$  is the solvent's flow time through the capillary (s);  $\eta_{sp}$  is the incremental viscosity;  $[\eta]$  is the characteristic viscosity (dL g<sup>-1</sup>); and  $c$  is the solution's concentration (g dL<sup>-1</sup>). The average molecular weight of PET was deduced from the measured characteristic viscosity.

Firstly:



Second:

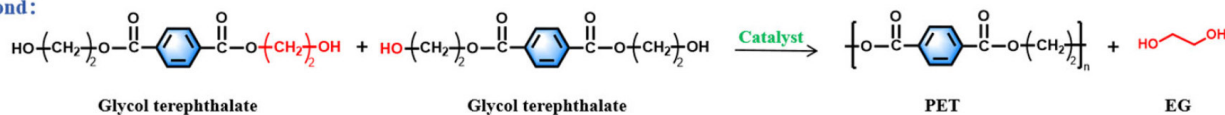


Figure 2. Preparation of PET

## RESULTS AND DISCUSSION

### Catalyst characterization

As shown in Figures 3 and 4, the scanning electron microscope test results of Ti-EG catalysts showed that the particle size distribution of Ti-EG was in the range of 0-30  $\mu\text{m}$ , with a cross-linked rhombic lamellar structure.

The scanning electron microscope test results of Si-EG catalysts showed that the particle size distribution of Si-EG was in the range of 0-400  $\mu\text{m}$ , and the surface was lumpy with obvious porous structure.

The test results showed that Ti-EG could be uniformly dispersed in EG for more than 60 min, and Si-EG could be uniformly dispersed in EG for more than 30 min, and both of them had good dispersibility in EG.

Figure 5 shows the X-ray diffractometer (XRD) patterns of the catalysts under different drying temperature treatments, it can be seen that there is no obvious change in the XRD patterns of Si-EG under drying treatments at 80 and 200  $^{\circ}\text{C}$ , and both of them do not show obvious peak shapes of  $\text{SiO}_2$  crystals, which can demonstrate that they did not decompose into  $\text{SiO}_2$ . Ti-EG exists with  $\text{Ti}_2\text{C}_2\text{H}_2\text{O}_8$  (PDF#48-1164) and  $\text{TiO}_2$  (PDF#76-1934) XRD crystal faces.

As can be seen in Figure 6, the peaks at 2798.1-2953.7  $\text{cm}^{-1}$  in the Fourier transform infrared spectroscopy (FTIR) spectrum of Ti-EG correspond to the  $-\text{CH}_2$  telescopic vibration, the strong absorption peak at 1047.3  $\text{cm}^{-1}$  corresponds to the telescopic vibration of the  $\text{Ti}-\text{O}-\text{C}$  bond, and the absorption peak at 590.1  $\text{cm}^{-1}$  corresponds to the  $\text{Ti}-\text{O}$  telescopic vibration.

Si-EG was dried at 80 and 200  $^{\circ}\text{C}$ . It was observed that the  $-\text{OH}$  stretching vibration at 3303.2  $\text{cm}^{-1}$  in the FTIR spectrum of Si-EG disappeared significantly at 200  $^{\circ}\text{C}$ , which could be attributed to the adsorption of incompletely reacted EG on the surface of the catalyst by the micropores. The absorption peaks at 792.1  $\text{cm}^{-1}$  corresponding to the  $\text{Si}-\text{O}-\text{C}$  bond and 1031.6  $\text{cm}^{-1}$  corresponding to the  $\text{Si}-\text{O}$  stretching vibration do not change much in the figure, which indicates that no thermal decomposition of Si-EG occurred.

As shown in Figure 7, the catalyst was hydrolyzed in deionized water at a constant temperature of 50  $^{\circ}\text{C}$ . The FTIR spectra of the catalyst were analyzed, and when the hydrolysis time of Ti-EG was 0.5 h, the presence of the absorption peak of the  $\text{Ti}-\text{O}$  bond was obviously strengthened, and the  $\text{Ti}-\text{O}-\text{C}$  was weakened, and the catalyst was hydrolyzed to  $\text{TiO}_2$ , and was poorly hydrolysis-resistant. The catalyst can only be used in the polycondensation stage.

The FTIR spectra of Si-EG hydrolyzed at different times showed

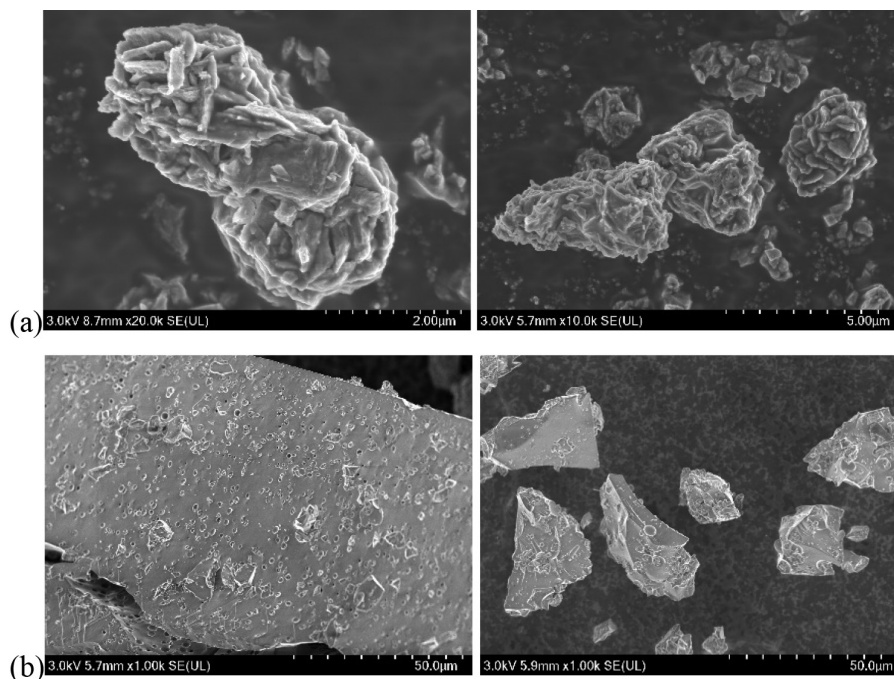


Figure 3. SEM of Ti-EG (a) and Si-EG (b)

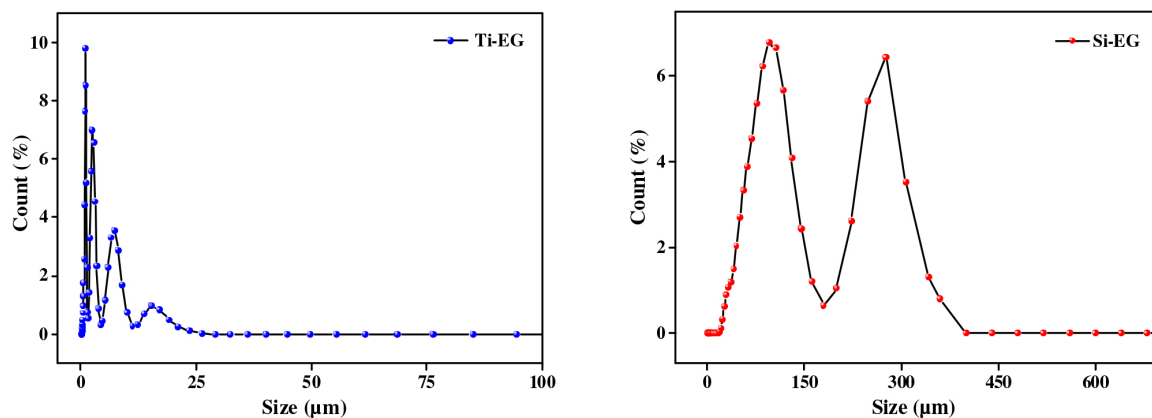


Figure 4. Particle size distribution of the catalyst

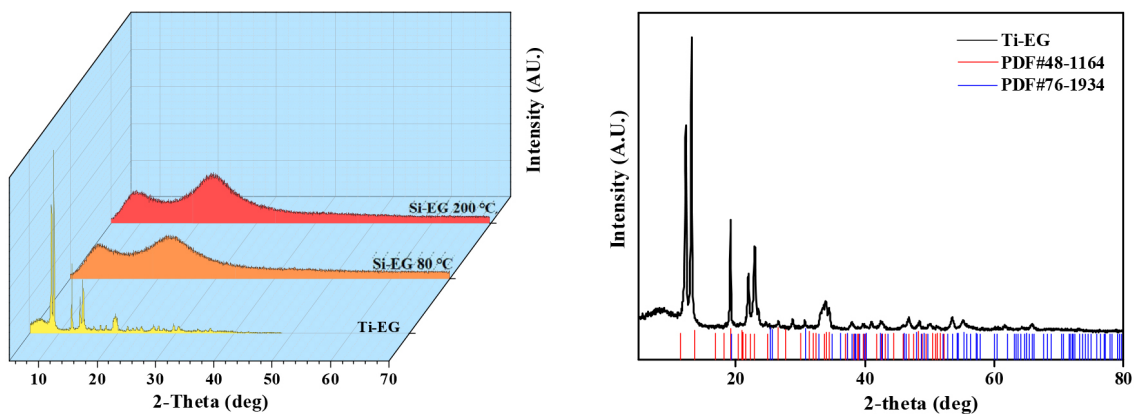


Figure 5. XRD spectra of catalysts

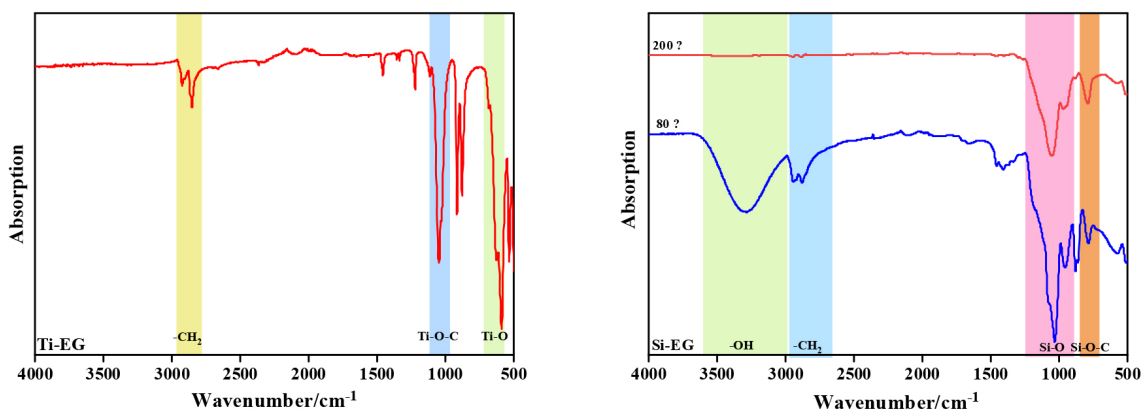


Figure 6. FTIR of the catalyst

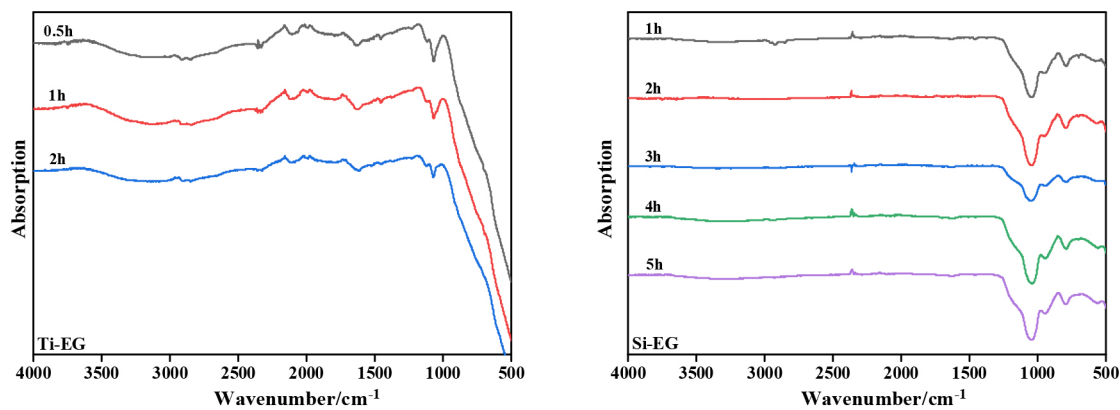


Figure 7. Hydrolytic stability test of catalyst

that the structure of Si-EG did not change significantly, the catalyst was not hydrolyzed, and its hydrolysis resistance was strong.

The thermogravimetric (TG) curve of Ti-EG shown in Figure 8 indicates that its weight loss is mainly concentrated around 350 °C. The catalysts are mainly used in the PET production. It meets the catalyst application conditions of 260-280 °C and will not thermally decompose during use.

The TG curve of Si-EG is divided into two weight loss stages. The first weight loss occurs before 200 °C, attributed to the adsorption of partially reacted glycol or solvent by the catalyst's porous structure. As the temperature increases, the second weight loss stage occurs near 350 °C, corresponding to the thermal decomposition temperature of Si-EG. This second thermal decomposition stage of Si-EG meets the usage conditions for condensation catalysts, necessitating a pre-use drying at 200 °C. Figures 5 and 6 also verify this view.

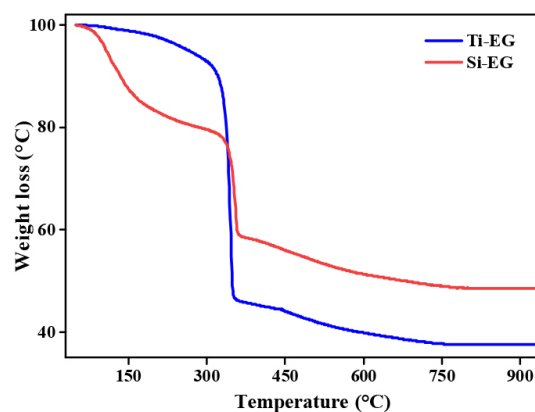


Figure 8. TG curves of Ti-EG and Si-EG

## Catalyst applications

Ti-EG and Si-EG were produced and used together. The molecular weight and color ( $b^*$ ) of PET were examined for Ti:Si at 1:0, 3:1, 2:1, 1:1, 1:2, 1:3, and 1:4 (mol).

It was experimentally verified that when Si-EG catalysts were used alone for PET catalysis, the molecular weight of the products was very low and the reaction was incomplete, so they were not considered for individual application.

The analysis of Figure 9 shows that, with the increase of the Ti:Si (mol) ratio, it can be found that when the  $b^*$  value of synthetic product PET gradually increases the yellow color tendency of PET is aggravated, and the molecular weight of synthetic PET also has a tendency to increase gradually but not significantly. However, as the proportion of Ti-EG is too high, the molecular weight of PET shows a decreasing trend, the  $b^*$  value of PET also increases significantly, and the yellow color deepens significantly. Considering that the increase of side reactions in the polycondensation stage led to the yellowing of PET color, the excessive side reactions caused PET to be capped prematurely in the polycondensation stage, which made it difficult to increase the molecular weight of PET. The highest  $b^*$  value of the synthesized PET was measured when all Ti-EG was used, and the molecular weight tended to decrease. As the ratio of Ti:Si (mol) decreases, a decreasing trend in both  $b^*$  value and molecular weight of PET can be observed. When Ti:Si is 1:4, the molecular weight of PET shows a significant decrease, which is caused by the insufficient catalytic activity of Si-EG. When Ti:Si is 1:1, the indexes of PET are more moderate and the overall quality is most excellent.

The FTIR spectrum of the synthesized PET is shown in Figure 10. The strong absorption peaks at 1650-1770  $\text{cm}^{-1}$  correspond to the

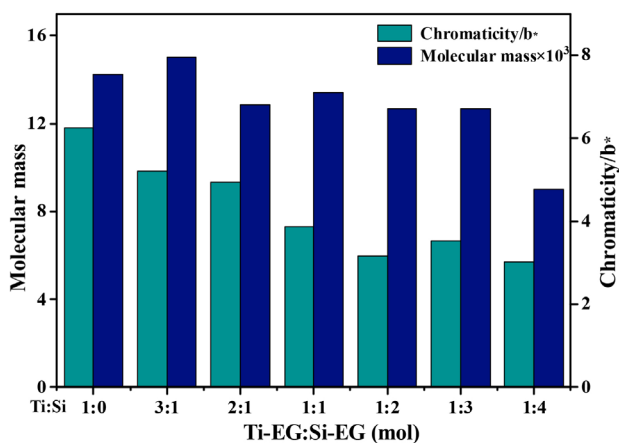


Figure 9. Effect of Ti:Si (mol) ratio on PET color ( $b^*$ ) and molecular weight

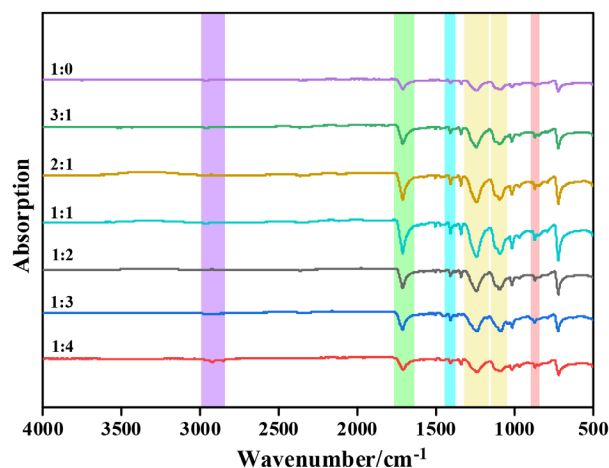
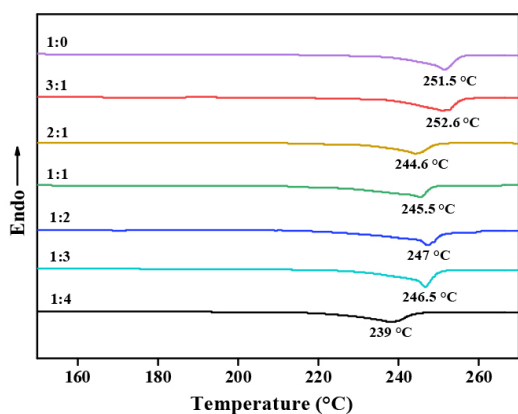


Figure 10. FTIR spectrum of PET

telescopic vibration of ester C=O, the aromatic  $\text{C-H}$  vibration peaks at 1390-1450  $\text{cm}^{-1}$ , the  $\text{C-O}$  vibration peaks at 1160-1300  $\text{cm}^{-1}$  and 1050-1150  $\text{cm}^{-1}$ , and the  $\text{C-O}$  vibration peaks at 850-890  $\text{cm}^{-1}$ . The  $\text{C-H}$  vibration of the methylene group in the EG chain was observed at 2850-2980  $\text{cm}^{-1}$ . The infrared spectra of the catalytic synthesized products were consistent with those of PET, which confirmed that the catalytic products were all PET.

It can be seen from the IR plot that the C=O and  $\text{C-O}$  absorption peaks in PET weakened with the increase of Ti ratio in the catalyst. This predicts that increasing the Ti ratio leads to very high catalyst activity, intensification of side reactions, and poor PET chain formation; the C=O and  $\text{C-O}$  bond absorption peaks are the strongest when the Ti:Si in the catalyst is 1 (mol), which predicts better PET molecular chain formation and moderate catalyst activity; and with the increase of Si ratio in the catalyst, it can be seen that C=O and  $\text{C-O}$  absorption peaks in PET are weakened again, which may predict that the activity of the catalyst is too low and the catalytic effect of the catalyst is incomplete, PET chain formation is weak.

The mass of the synthesized PET sample was weighed at about 8-10 mg, the flow rate of nitrogen was 40  $\text{mL min}^{-1}$ , and the programmed temperature started from  $-10$   $^{\circ}\text{C}$  at a rate of 10  $^{\circ}\text{C min}^{-1}$  to 280  $^{\circ}\text{C}$ , kept warm for 10 min, and then reduced the temperature to  $-10$   $^{\circ}\text{C}$  at a rate of 10  $^{\circ}\text{C min}^{-1}$ , then kept warm for 10 min.

The differential scanning calorimetry (DSC) curves of the measured PET samples are shown in Figure 11. The melting and crystallization temperatures of the synthesized PET showed a decreasing trend as the Ti:Si (mol) ratio decreased. However, when all Ti-EG was used for PET catalysis, it can be seen that the melting and crystallization temperatures of PET were not the

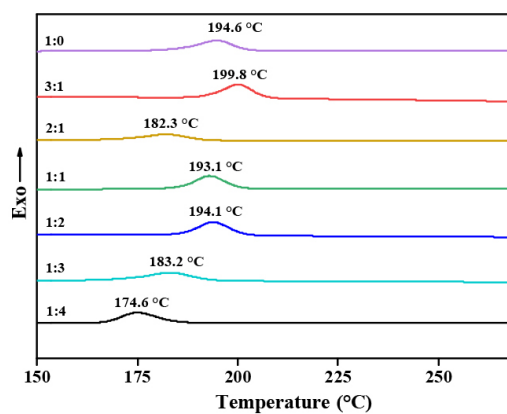


Figure 11. DSC curves of synthesized PET with different Ti:Si ratio

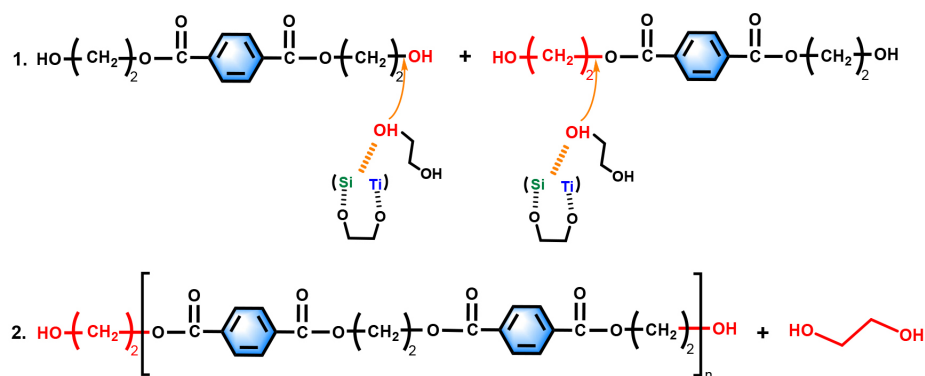


Figure 12. Reaction mechanisms

highest, which is considered to be due to the accumulation of side-reaction products caused by the catalytic process, thus leading to the deterioration of the molecular chain regularity and crystalline properties of the samples.

### Reaction mechanisms

As shown in Figure 12, the mechanism of catalyst action is that the catalysts Ti, Si, and O synergistically activate the hydroxyl groups at the ends of the ethylene glycol and attack the two ester groups at the ends of the ethylene terephthalate, so that the hydroxyl group (–OH) and the hydroxyethyl group (–CH<sub>2</sub>CH<sub>2</sub>OH) at the ends of the ethylene terephthalate are bond-breakingly removed and bonded to form a new EG.

The polycondensation stage is the process of repeating the above process to finally synthesize large molecular weight PET.

### CONCLUSIONS

In this study, the performance of Ti and Si catalysts with different ratios was compared and analyzed under the same conditions of use, and the optimum ratio of Ti and Si glycol salt catalysts when used together was investigated. The study clearly shows the effect of Ti, and Si on the catalytic activity at different ratios. The polycondensation temperature was 260–280 °C, the polycondensation pressure was –0.1 MPa, the polycondensation time was 60 min, and the total amount of catalyst added was 0.015% of the raw material. By testing the thermal properties, molecular weight, and color (*b*<sup>\*</sup>) value of the prepared PET, it can be concluded that the color (*b*<sup>\*</sup>) of the product PET was significantly reduced when Ti-EG was combined with Si-EG compared with a single Ti-EG. The performance of PET prepared with titanium:silicon ratio of 1:1 (mol) is moderate. This proves that the simultaneous use of Si-EG and Ti-EG can effectively reduce the catalytic activity of Ti-EG catalysts, the catalytic activity of the catalyst is moderate and the quality of PET produced is better under the joint action of the two catalysts. Both Si-EG and Ti-EG can be uniformly dispersed into ethylene glycol, and since Si-EG has a stable inert porous structure and a physical adsorption effect on Ti-EG, it makes the catalyst have a good color (*b*<sup>\*</sup>). Physical adsorption, which makes the catalyst show better catalytic performance and catalytic stability under the joint action of the two catalysts, can effectively reduce the Lewis acidity of titanium and regulate its catalytic activity for PET. This study provides a reference for adjusting and changing the catalyst activity by adjusting the combination ratio of titanium and silicon elements to produce environmentally friendly and efficient PET polycondensation catalysts.

### ACKNOWLEDGMENTS

Thanks to all the authors for their efforts in completing this manuscript.

### REFERENCES

- Shimamoto, G. G.; Kazitoris, B.; de Lima, L. F. R.; de Abreu, N. D.; Salvador, V. T.; Bueno, M.; de Castro, E. V. R.; Silva Filho, E. A.; Romao, W.; *Quim. Nova* **2011**, *34*, 1389. [Crossref]
- Zhao, Y. B.; Lv, X. D.; Ni, H. G.; *Chemosphere* **2018**, *209*, 707. [Crossref]
- Pellis, A.; Acero, E. H.; Gardossi, L.; Ferrario, V.; Guebitz, G. M.; *Polym. Int.* **2016**, *65*, 861. [Crossref]
- Espinosa-Lopez, A. C.; Avila-Orta, C. A.; Medellin-Rodriguez, F. J.; Gonzalez-Morones, P.; Gallardo-Vega, C. A.; de Leon-Martinez, P. A.; Navarro-Rosales, M.; Valdez-Garza, J. A.; *Polym. Bull.* **2019**, *76*, 2931. [Crossref]
- Shen, G. L.; Ning, G. L.; *Adv. Mater. Res.* **2012**, *4*, 6381. [Crossref]
- Santiago-Portillo, A.; Navalon, S.; Alvaro, M.; Garcia, H.; *J. Catal.* **2018**, *365*, 450. [Crossref]
- De Clercq, R.; Dusselier, M.; Poleunis, C.; Debecker, D. P.; Giebler, L.; Oswald, S.; Makshina, E.; Sels, B. F.; *ACS Catal.* **2018**, *8*, 8130. [Crossref]
- Yu, Y. K.; Wang, R.; Liu, W.; Chen, Z.; Liu, H. X.; Huang, X.; Tang, Z. M.; Liu, Y. M.; He, M. Y.; *Appl. Catal., A* **2021**, *610*, 117953. [Crossref]
- Santulli, F.; D'Auria, I.; Boggioni, L.; Losio, S.; Proverbio, M.; Costabile, C.; Mazzeo, M.; *Organometallics* **2020**, *39*, 1213. [Crossref]
- Xiao, B.; Wang, L. P.; Mei, R. H.; Wang, G. Y.; *Chin. Chem. Lett.* **2011**, *22*, 741. [Crossref]
- Satoto, R.; Morikawa, J.; Hashimoto, T.; *J. Therm. Anal. Calorim.* **2002**, *70*, 713. [Crossref]
- Song, F.; Liu, Y. M.; Wang, L. L.; Zhang, H. J.; He, M. Y.; Wu, P.; *Stud. Surf. Sci. Catal.* **2007**, *170*, 1236. [Crossref]
- Wen, R. Y.; Shen, G. L.; Yu, Y.; Xu, S. J.; Wei, J.; Huo, Y.; Jiang, S. J.; *RSC Adv.* **2023**, *13*, 17166. [Crossref]
- Wen, R. Y.; Shen, G. L.; Zhai, J. M.; Meng, L. H.; Bai, Y. L.; *New J. Chem.* **2023**, *47*, 14646. [Crossref]
- Yamamoto, K.; Shimoita, H.; Tomita, K.; Fujita, K.; Kobayashi, M.; Petrykin, V.; Kakihana, M.; *J. Ceram.* **2009**, *117*, 347. [Crossref]
- Tang, R. Z.; Chen, T.; Chen, Y.; Zhang, Y. Z.; Wang, G. Y.; *Chin. J. Catal.* **2014**, *35*, 457. [Crossref]
- Cheng, H.; Lin, K. L.; Cui, R.; Hwang, C. L.; Chang, Y. M.; Cheng, T. W.; *Constr. Build. Mater.* **2015**, *95*, 710. [Crossref]
- Zhao, H.; Yin, X.; Wang, Y. H.; *Diamond Relat. Mater.* **2022**, *127*, 109195. [Crossref]
- Liu, Z. J.; Liu, Z. M.; Ji, S.; Wang, G. S.; *Sci. Rep.* **2020**, *10*, 16750. [Crossref]

20. Guo, Y. J.; Hwang, S. J.; Katz, A.; *Mol. Catal.* **2019**, *477*, 110509. [Crossref]
21. Hirakata, H.; Kawai, T.; Kondo, T.; Minoshima, K.; *Mater. Sci. Eng., A* **2018**, *737*, 105. [Crossref]
22. Ykrelef, A.; Nadji, L.; Issaadi, R.; Agouram, S.; *Catal. Today* **2018**, *299*, 93. [Crossref]
23. Yin, M.; Feng, R. C.; Li, C. C.; Guan, G. H.; Zhang, D.; Xiao, Y. N.; *Chem. J. Chin. Univ.* **2010**, *31*, 418. [Link] accessed in March 2024
24. Yu, Y.; Shen, G.; Xu, T. J.; Wen, R.; Qiao, Y. C.; Cheng, R. C.; Huo, Y.; *RSC Adv.* **2023**, *13*, 36337. [Crossref]
25. Belowich, M. E.; Roberts, J. M.; Peterson, T. H.; Bellinger, E.; Syverud, K.; Sidle, T.; *Macromolecules* **2020**, *53*, 7487. [Crossref]
26. Salazar-Hernandez, C.; Cervantes, J.; Alonso, S.; *J. Sol-Gel Sci. Technol.* **2010**, *54*, 77. [Crossref]
27. El-Toufaily, F. A.; Wiegner, J. P.; Feix, G.; Reichert, K. H.; *Thermochim. Acta* **2005**, *432*, 99. [Crossref]
28. Konstantopoulou, M.; Terzopoulou, Z.; Nerantzaki, M.; Tsagkalias, J.; Achilias, D. S.; Bikiaris, D. N.; Exarhopoulos, S.; Papageorgiou, D. G.; Papageorgiou, G. Z.; *Eur. Polym. J.* **2017**, *89*, 349. [Crossref]
29. Geng, Y. H.; Sui, Y.; *Acta Polym. Sin.* **2019**, *50*, 109. [Crossref]
30. Hao, T. Z.; Chen, Y. H.; Li, L. L.; Xuan, P.; *Acta Polym. Sin.* **2022**, *53*, 1057. [Crossref]
31. Cheng, H. D.; Chen, S. J.; *Progress in Chemistry* **2017**, *29*, 443. [Crossref]
32. Xu, Q.; Ji, T.; Tian, Q.; Su, Y.; Niu, L.; Li, X.; Zhang, Z.; *Nano* **2018**, *13*, 1. [Crossref]
33. Clingerman, D.; *CoatingsTech* **2021**, *18*, 32. [Link] accessed in March 2024